

H^* Peusner's Form of the Kedem–Katchalsky Equations for Non-homogenous Non-electrolyte Binary Solutions

Izabella Ślęzak-Prochazka¹ · Kornelia M. Batko² ·
Sławomir Wąsik³ · Andrzej Ślęzak⁴

Received: 19 February 2015 / Accepted: 12 November 2015 / Published online: 1 December 2015
© The Author(s) 2015. This article is published with open access at Springerlink.com

Abstract The paper presents a hybrid matrix form of Kedem–Katchalsky equations that contains Peusner's coefficients H_{ij}^* ($i, j = 1, 2$) for the conditions of concentration polarization and H_{ij} for homogeneous solutions. The aqueous glucose solutions were analyzed in Nephrophan membrane system with membrane in horizontal plane. The calculations of coefficients H_{ij}^* were made for the *A* and *B* configurations of the membrane system. In the *A* configuration glucose solution with higher concentration was located below and the solution with lower concentration above the membrane. In configuration *B* locations of the solutions were reversed. Non-diagonal coefficients of matrix $[H^*]$ (concentration polarization conditions) were shown to be linearly dependent on average concentration of glucose solution in the membrane. H_{12}^* in *A* configuration was lower than in *B* configuration. Non-diagonal coefficients of matrix $[H^*]$ were lower than appropriate coefficients of matrix $[H]$ (homogeneous solutions). For diagonal coefficients of matrix $[H^*]$ coefficient H_{11}^* is constant and equal to H_{11} , whereas H_{22}^* and H_{22} are non-linearly dependent on average concentration of glucose solution in the membrane. Value

✉ Kornelia M. Batko
kornelia.batko@ue.katowice.pl

Izabella Ślęzak-Prochazka
izabella.slezak-prochazka@polsl.pl

Sławomir Wąsik
s.wasik@ujk.edu.pl

Andrzej Ślęzak
aslezak52@gmail.com

¹ Biosystems Group, Institute of Automatic Control, Silesian University of Technology, 2A Akademicka, 44100 Gliwice, Poland

² Department of Informatics for Economics, University of Economics, 2B Bogucicka, 40287 Katowice, Poland

³ Institute of Physics, Jan Kochanowski University, 15 Świętokrzyska, 25509 Kielce, Poland

⁴ Department of Public Health, Częstochowa University of Technology, 36b Armia Krajowa, 42200 Czestochowa, Poland

of H_{22}^* in A was lower than in B configuration of the membrane system. Additionally, H_{22}^* were lower than H_{22} . For both A and B configurations and concentration polarization conditions, the coefficients H_{12}^* and H_{22}^* of matrix $[H^*]$ are different for average solution concentrations $>5.41 \text{ mol m}^{-3}$ due to convective mixing of solutions in B configuration.

Keywords Membrane transport · Peusner's network thermodynamics · Matrix form of hybrid Kedem–Katchalsky equations · Concentration polarization · H_{ij} hybrid coefficients

List of symbols

R_{ij}, L_{ij}	Symmetric Peusner's coefficients for homogeneous solutions
P_{ij}, H_{ij}	Hybrid Peusner's coefficients for homogeneous solutions
X_i	Thermodynamic forces in homogeneous conditions
J_i	Thermodynamic fluxes in homogeneous conditions
R_{ij}^*, L_{ij}^*	Symmetric Peusner's coefficients for non-homogeneous solutions
P_{ij}^*, H_{ij}^*	Hybrid Peusner's coefficients for non-homogeneous solutions
X_i^*	Thermodynamic forces in non-homogeneous conditions
J_i^*	Thermodynamic fluxes in non-homogeneous conditions
L_p	Hydraulic permeability coefficient
J_v	Volume flux in homogeneous conditions
J_{vs}	Volume flux in non-homogeneous conditions
σ	Reflection coefficient
ω	Solute permeability coefficient
ν	Kinematic viscosity
ρ	Mass density of solution
δ_A, δ_B	Thickness of concentration boundary layers in configurations A and B of membrane system
P_h, P_l	Hydrostatic pressure (h higher and l lower value)
$\Delta\pi$	Osmotic pressure difference
ΔP	Hydrostatic pressure difference
C_h, C_l	Solute concentrations in chambers of the membrane system
\bar{C}	Mean solute concentration in the membrane
R	Gas constant
R_C	Concentration Rayleigh number
T	Thermodynamic temperature
D_A, D_B	Diffusion coefficient in configurations A and B
ζ_p	Hydraulic concentration polarization coefficient
ζ_v	Osmotic concentration polarization coefficient
ζ_s	Diffusive concentration polarization coefficient
ζ_a	Advective concentration polarization coefficient
κ_{ij}	Asymmetry factor between configurations A and B
χ_{ij}	Concentration polarization coefficient

1 Introduction

Peusner's Network Thermodynamics (Peusner's NT) is one of the methods used to describe transport in membrane systems that enables symmetrical and/or hybrid transformation of classical Kedem–Katchalsky equations to network forms (Peusner 1970, 1983, 1985, 1986). For homogeneous binary non-electrolyte solutions there are two symmetrical and two hybrid forms of network K–K equations. The symmetrical forms of these equations contain Peusner's coefficients R_{ij} or L_{ij} and hybrid forms—Peusner's coefficients P_{ij} and H_{ij} (Peusner 1983, 1986; Batko et al. 2013). These coefficients appear in matrix form of the phenomenological equations. The coefficients L_{ij} and R_{ij} derive directly from the Onsager's phenomenological equation. The introduction of the coefficients P_{ij} and H_{ij} is a consequence of application of network thermodynamics techniques.

The assumption of homogeneity of the solutions separated by a membrane is satisfied only when solutions of different concentrations separated by a membrane are homogeneous (thoroughly mixed by mechanical stirring) (Katchalsky and Curran 1965; Ślęzak 1989). If these solutions are not mechanically stirred, the concentration boundary layers (CBL) are formed on both sides of artificial and/or biological membranes. The formation of CBL is an important process that occurs in the technical and biological systems (Barry and Diamond 1984; Shachar-Hill and Hill 1993; Larchet et al. 2008; Pappenheimer 2001; Grzegorzczyn et al. 2008; Mishchuk 2010; Nikonenko et al. 2010; Grzegorzczyn and Ślęzak 2012; Wang et al. 2014). These layers change the concentration gradient through the membrane and serve as additional kinetic barriers to the fast permeating substances and, in result, reduce the values of the volume and solute fluxes (Abu-Rjal et al. 2014; Barry and Diamond 1984; Ślęzak 1989; Dworecki 1995; Dworecki et al. 2003, 2005; Kargol 2000; Ślęzak et al. 1985, 2010). The processes of creation and destruction of CBLs may be visualized by optical methods (Dworecki 1995; Fernández-Sempere et al. 2009; Salcedo-Diaz et al. 2014).

In our previous papers (Ślęzak et al. 2012a, b; Batko et al. 2014a, b, 2015) network forms of the Kedem–Katchalsky equations were applied to interpret the transport of binary non-electrolyte solutions through horizontally mounted membrane in concentration polarization conditions. The coefficients L_{ij}^* , R_{ij}^* and P_{ij}^* ($i, j \in \{1, 2\}$) were calculated for aqueous solutions of glucose and polymer membrane. Additionally, the values of coefficients L_{ij}^* , R_{ij}^* and P_{ij}^* were compared to the values of coefficients L_{ij} , R_{ij} and P_{ij} calculated for conditions of solution homogeneity for the same values \bar{C} and two configurations of membrane system. There was a threshold value of concentration (\bar{C}_{cr}) and only for $\bar{C} > \bar{C}_{cr}$ the coefficients L_{ij}^* , R_{ij}^* and P_{ij}^* were dependant on the membrane system configuration. It was also shown that for $\bar{C} > \bar{C}_{cr}$ coefficients relations L_{ij}^*/L_{ij} , R_{ij}^*/R_{ij} and P_{ij}^*/P_{ij} depended on a membrane system configuration.

In the present paper, Kedem–Katchalsky equations were transformed into hybrid matrix form and applied to interpret the membrane transport of non-electrolyte solutions in conditions of concentration polarization. We assessed the influence of the concentration polarization on the value of Peusner's coefficients H_{ij}^* , for aqueous solutions of glucose and a Nephrophan hemodialysis membrane. The values of these coefficients were compared to the values of coefficients H_{ij} calculated for the same concentrations of homogeneous solutions and different configurations of the membrane. To find new coefficients better describing the membrane transport in concentration polarization conditions for both configurations of the membrane system, we analyzed other combinations of coefficients of matrixes $[H^*]$ and $[H]$ for A and B configurations.

2 Theory

Similar to the previous papers (Ślęzak et al. 2012a,b; Batko et al. 2014a,b, 2015), let us consider a single-membrane system schematically presented in Fig. 1, in which an electroneutral, selective polymer membrane (M) separates two non-homogeneous (mechanically unstirred) binary non-electrolyte solutions with concentrations C_l and C_h ($C_l < C_h$) at the initial moment ($t = 0$). The membrane transport processes are isothermal and stationary, and no chemical reaction occurs in the solutions separated by membrane. According to the Kedem and Katchalsky formalism, the membrane is characterized by the hydraulic permeability (L_p), reflection (σ) and solute permeability (ω) coefficients (Kedem and Katchalsky 1958). The values of these coefficients do not depend on the configuration of the membrane system (Ślęzak 1989).

As shown in Fig. 1, for a single-membrane system with a horizontally oriented membrane, configurations A and B may be distinguished (Ślęzak 1989; Batko et al. 2014a,b). In this system, water and dissolved substance that diffuse through the membrane form the concentration boundary layers (CBL) l_l and l_h on both sides of the membrane. The layers l_l and l_h are treated as pseudomembranes, and their thicknesses are denoted by δ_l and δ_h (Ślęzak et al. 1985, 2005, 2010). In configuration A, solutions with concentration C_l and C_h are located in the compartments above and below the membrane, respectively, and their thicknesses are denoted by $\delta_l = \delta_h = \delta_A = \delta_d$. In this configuration the layers of higher density are under layers with lower density (Ślęzak et al. 1985; Ślęzak 1989). The structure of layers l_l and l_h is gravitationally stable, since the density gradient in CBLs is parallel to the vector of gravity (\vec{g}) (Ślęzak et al. 1985; Dworecki et al. 2005). Thus in configuration A only diffusive transport occurs and the diffusion process is characterized by diffusion coefficient $D_l = D_h = D_A = D_d$ (Ślęzak et al. 1985; Dworecki et al. 2005).

In the configuration B, solutions with concentrations C_l and C_h are placed inversely relative to the membrane mounted horizontally and the density gradient in CBL is anti-parallel to the vector of gravity. In this configuration the CBL of higher density are above CBL with lower density. Although the density gradient is antiparallel to \vec{g} , a layer system in this configuration is stable, since the viscous forces prevent vertical movement of the solutions. This means that

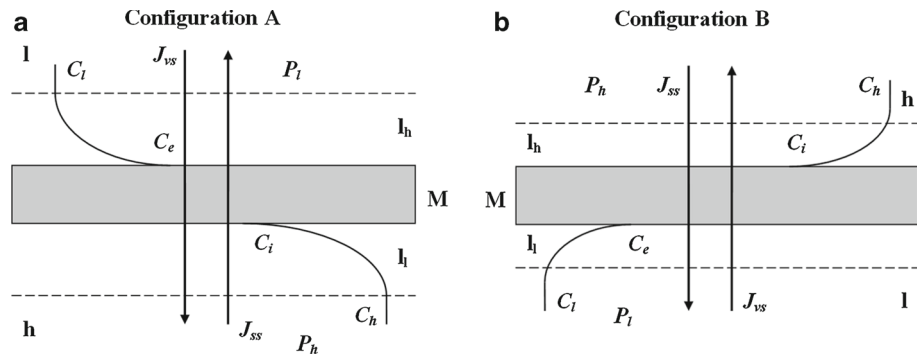


Fig. 1 Configurations A and B of a single-membrane system: M—membrane; l_l and l_h —the concentration boundary layers (CBLs), P_h and P_l —mechanical pressures; C_l and C_h —concentrations of solutions outside the boundaries; C_e and C_i —the concentrations of solutions at boundaries l_l/M and M/l_h ; J_{vm} —the volume fluxes through membrane M; J_{vs} —the volume fluxes through complex $l_l/M/l_h$; J_{sl} , J_{sh} and J_{sm} —the solute fluxes through layers l_l , l_h and membrane, respectively; J_{ss} —the solute fluxes through complex $l_l/M/l_h$ (Ślęzak et al. 2012a,b).

at small difference of concentrations the viscosity prevails, the solution remains in a stable state, and the substance is transported by diffusion. In this steady state all concentration fluctuations, the same as the liquid density fluctuations, are suppressed. The transition from stable to unstable state occurs when the buoyant forces are larger than the viscous forces. In this moment, convective transport occurs in addition to diffusion. In convective state, liquid non-active state is unstable relative to any small disturbance. This process is a membrane version of the Rayleigh–Benard–Taylor phenomenon (Ślęzak et al. 1985; Dworecki et al. 2005; Grzegorzczyn and Ślęzak 2012). In this configuration, both diffusive and diffusive–convective conditions may occur. This indicates that the membrane transport process is characterized by diffusion coefficient (D_d) and convective diffusion coefficient (D_{dk}). In general, for configurations A and B we assume that $D_r = D_d + D_{dk}$ ($r = A$ or B). In configuration A and B (for $\bar{C} < \bar{C}_{cr}$), $D_A = D_B = D_d$ and $D_{dk} = 0$ and in configuration B for $\bar{C} \geq \bar{C}_{crit.}$, $D_B = D_d + D_{dk}$ and $D_{dk} > D_d$. Additionally $\delta_B = \delta_{dk}$ and $\delta_{dk} < \delta_d$.

For concentration polarization conditions we denote the concentrations of solutions at boundaries l_l/M and M/l_h by C_e and C_i ($C_e < C_i$, $C_e > C_l$, $C_i < C_h$), respectively. We assume that the mass density (ρ) of the solutions of concentrations C_l , C_e , C_i and C_h fulfills the condition $\rho_l < \rho_e < \rho_i < \rho_h$. The thickness (δ) is a basic parameter of CBL (Schlichting and Gersten 2000) that can be evaluated by the optical (Dworecki 1995; Nikonenko et al. 2010) and the volume or solute fluxes methods (Barry and Diamond 1984; Ślęzak et al. 2010; Jasik-Ślęzak et al. 2011). In certain hydrodynamic conditions CBLs can be partially destroyed by natural convection (Dworecki et al. 2005; Nield and Bejan 2006). This process limits the growth of thickness δ_l and δ_h of the layers l_l and l_h to critical values $(\delta_l)_{cr}$ and $(\delta_h)_{cr}$ and accelerates diffusion of substances outside the layers (Ślęzak et al. 1985; Dworecki et al. 2005). The transport parameters of layers l_l and l_h are characterized by the solute permeability coefficients: $\omega_l = D_l(RT\delta_l)^{-1}$ and $\omega_h = D_h(RT\delta_h)^{-1}$, where D_l and D_h are the diffusion coefficients in layers l_l and l_h , respectively (Katchalsky and Curran 1965). The solute permeability coefficient of complex $l_l/M/l_h$ is denoted by ω_s . The following relation between coefficients D_l , ω , D_h , δ_l , δ_h and ω_s is fulfilled $\omega^{-1} + RT(\delta_l D_h + \delta_h D_l) D_l^{-1} D_h^{-1} = \omega_s^{-1}$ (Katchalsky and Curran 1965; Demirel 2007).

The development of natural convection process is controlled by a concentration Rayleigh number (R_C) that characterizes loss of stability (Ślęzak et al. 1985; Dworecki et al. 2005). Hydrodynamic stability of CBL in membrane systems is controlled by the concentration Rayleigh number (R_C), which may be written in the following form (Dworecki et al. 2005)

$$R_C = \frac{gRT\omega\delta^4\alpha_C(C_h - C_l)}{\nu D(D + 2RT\omega\delta)} = \frac{gRT\omega\delta^4\alpha_C\bar{C} \ln(C_h C_l^{-1})}{\nu D(D + 2RT\omega\delta)} \tag{1}$$

where g —the gravitational acceleration, δ —thickness of the CBL, $\alpha_C = (\partial\rho/\partial C)/\rho$ —variation of density with the concentration, ρ —mass density, D —diffusion coefficient of the solute and ν —the kinematic viscosity of the fluid. The value of R_C depends on the gravity acceleration, concentration, viscosity and density of the transported solutions (Dworecki et al. 2005; Jasik-Ślęzak et al. 2011; Ślęzak et al. 2010). For configuration B , when the value of R_C reaches a critical value $(R_C)_{cr}$, transition from non-convective (stable) to the convective (unstable) state is observed. $(R_C)_{cr}$ is reached at the bifurcation point. In the previous paper (Ślęzak et al. 2010) it was shown that the critical value of concentration Rayleigh number $(R_C)_{cr} = 1709.3$ was reached for $\bar{C}_{cr} = 5.41 \text{ mol m}^{-3}$. $(R_C)_{cr}$ is the limit of the stability of membrane system relative to any concentration (density) disturbance (Landau and Lifshitz 1987).

For the $R_C > (R_C)_{cr}$ the hydrodynamic instability leads to the natural convection which reduces the thickness of CBL and increases the value of concentration gradient of the mem-

brane and consequently volume and solute fluxes (Ślęzak et al. 2010). The existence of such regulatory mechanism at the presence of a gravitational field justifies amplification and rectification of the volume and solute fluxes (Kargol 1992; Ślęzak 1989; Jasik-Ślęzak et al. 2011; Ślęzak et al. 2012a, b). These effects occur in single- and double-membrane systems containing binary or ternary solutions in conditions of concentration polarization when the density gradient in CBL formed in surroundings of horizontally mounted membrane is anti-parallel to the vector of gravity (Kargol 1992; Ślęzak 1989; Ślęzak et al. 2012a, b). In these conditions, the process of turbulent natural convection develops until the dendric-type structure called “plum structure” is formed (Puthenveetil and Arakeri 2008; Puthenveetil et al. 2011; Ramareddy and Puthenveetil 2011). Compactness of “plum structure” increases with increasing value of the R_C number (Puthenveetil and Arakeri 2008).

Noteworthy, the formation of the spatial structure of liquid instability phenomenon known as Rayleigh–Benard phenomenon has several versions. The earliest known version discovered by Bernard is caused by thermoconvection between a heated and a not non-heated plate (Normand et al. 1977). Later different version of the spatial structure of the liquid caused by electroconvection was observed due to electric field applied between the horizontally mounted electrodes (Baranowski and Kawczyński 1972; Baranowski 1980; Ward and Le Blanc 1984; Han and Grier 2005, 2006, 2012). Recently, studies focus mainly on electroconvection between the horizontally mounted electrodes separated by an ion exchange membrane (Larchet et al. 2008; Rubinstein and Zaltzman 2000; Moya and Horno 2004; Nikonenko et al. 2010; Serna et al. 2014).

The Bernard phenomenon and its electrochemical and membrane counterparts occur in similar circumstances: Despite increase in the value of the control parameter in conditions that are close to the position of the equilibrium, the membrane system is stable, since in these conditions stable state corresponds to the minimum entropy production. The system loses stability after reaching the critical value at the bifurcation point, and it may lead to conditions sufficient to initiate all irreversible processes that may occur in the system (Kondepudi and Prigogine 1981; Prigogine 1997). In addition to the bifurcation point, a class of phenomena appears that is classified as dissipative structures. This means that the matter gains new properties, in which the main role is played by fluctuations and instabilities, since entropy production generally increases in systems far from equilibrium (Prigogine 1997; Kondepudi 2008).

A hybrid equation is a source of coefficients H_{ij}^* under the conditions of concentration polarization, for a bi-directional two-port of Peusner’s NT with single input force X_1 and conjugate flux J_1^* and a single output flux J_2^* and force X_2

$$\begin{bmatrix} X_1 \\ J_2^* \end{bmatrix} = \begin{bmatrix} H_{11}^* & H_{12}^* \\ H_{21}^* & H_{22}^* \end{bmatrix} \begin{bmatrix} J_1^* \\ X_2 \end{bmatrix} = [H^*] \begin{bmatrix} J_1^* \\ X_2 \end{bmatrix} \tag{2}$$

For the conditions of homogeneity of solutions separated by the membrane, the above equation can be rewritten as (Peusner 1983, 1985, 1986)

$$\begin{bmatrix} X_1 \\ J_2 \end{bmatrix} = \begin{bmatrix} H_{11} & H_{12} \\ H_{21} & H_{22} \end{bmatrix} \begin{bmatrix} J_1 \\ X_2 \end{bmatrix} = [H] \begin{bmatrix} J_1 \\ X_2 \end{bmatrix} \tag{3}$$

For the conditions of concentration polarization, the K–K equations can be written as (Ślęzak et al. 2010)

$$\begin{bmatrix} J_{vs} \\ J_{ss} \end{bmatrix} = \begin{bmatrix} \zeta_p L_p & -\zeta_p L_p \zeta_v \sigma \\ \zeta_p L_p (1 - \zeta_a \sigma) \bar{C} & \zeta_s \omega - \zeta_p L_p \zeta_v \sigma (1 - \zeta_a \sigma) \end{bmatrix} \begin{bmatrix} \Delta P \\ \Delta \pi \end{bmatrix} \tag{4}$$

where J_{vs} is a volume and J_{ss} is a solute flux under the conditions of concentration polarization; $\zeta_p, \zeta_v, \zeta_a$ and ζ_s are hydraulic, osmotic, advective and diffusive Katchalsky's coefficients, respectively; L_p, σ and ω are the coefficients of hydraulic permeability, reflection and solute permeability for membrane, respectively; $\Delta P = P_h - P_l$ is the hydrostatic pressure difference (P_h, P_l are the higher and lower value of hydrostatic pressure; if pressure P_h is applied to the chamber with higher concentration (C_h), then $\Delta P > 0$); $\Delta\pi = RT(C_h - C_l)$ is the osmotic pressure difference (RT is the product of the gas constant and absolute temperature, C_h and C_l ($C_h > C_l$) are the solution concentrations; $\bar{C} = (C_h - C_l)[\ln(C_h C_l^{-1})]^{-1}$ is the average solutions concentration in the membrane).

By transforming Eqs. (2) and (4) for suitable forces $X_1 = \Delta P - \Delta\pi, X_2 = \Delta\pi/\bar{C}$ and fluxes $J_1^* = J_{vs}$ and $J_2^* = J_{ss}$ for the system $l_l/M/l_h$ we obtain

$$\begin{bmatrix} \Delta P - \Delta\pi \\ J_{ss} \end{bmatrix} = \begin{bmatrix} \frac{1}{\zeta_p L_p} & -(1 - \zeta_v \sigma)\bar{C} \\ (1 - \zeta_a \sigma)\bar{C} & \bar{C}\zeta_s \omega \end{bmatrix} \begin{bmatrix} J_{vs} \\ \frac{\Delta\pi}{\bar{C}} \end{bmatrix} = \begin{bmatrix} H_{11}^* & H_{12}^* \\ H_{21}^* & H_{22}^* \end{bmatrix} \begin{bmatrix} J_{vs} \\ \frac{\Delta\pi}{\bar{C}} \end{bmatrix} \quad (5)$$

From Eq. (5) for selective membrane ($0 < \sigma < 1$) it can be obtained $H_{11}^* = \zeta_p^{-1} L_p^{-1}, H_{12}^* = -(1 - \zeta_v \sigma)\bar{C} \neq H_{21}^* = \bar{C}(1 - \zeta_a \sigma)$ and $H_{22}^* = \bar{C}\zeta_s \omega$. This means that in the Eq. (6), the symmetry relation $H_{12}^* = H_{21}^*$ is not fulfilled. For unselective membrane we can write $H_{11}^* = (\zeta_p L_p)^{-1}, H_{12}^* = H_{21}^* = \bar{C}$ and $H_{22}^* = \bar{C}\zeta_s \omega$. In this case for semipermeable membrane $H_{11}^* = \zeta_p^{-1} L_p^{-1}, H_{12}^* = H_{21}^* = H_{22}^* = 0$. The determinant of matrix $[H^*]$ is equal

$$\det[H^*] = \bar{C} \left[\frac{\zeta_s \omega}{\zeta_p L_p} + \bar{C}(1 - \zeta_v \sigma)(1 - \zeta_a \sigma) \right] \quad (6)$$

In the homogeneity conditions of solution separated by selective membrane, i.e., when the condition $\zeta_p = \zeta_v = \zeta_a = \zeta_s = 1$ is fulfilled, Eq. (5) can be expressed as

$$\begin{bmatrix} \Delta P - \Delta\pi \\ J_s \end{bmatrix} = \begin{bmatrix} \frac{1}{L_p} & -(1 - \sigma)\bar{C} \\ (1 - \sigma)\bar{C} & \bar{C}\omega \end{bmatrix} \begin{bmatrix} J_v \\ \frac{\Delta\pi}{\bar{C}} \end{bmatrix} = \begin{bmatrix} H_{11} & H_{12} \\ H_{21} & H_{22} \end{bmatrix} \begin{bmatrix} J_v \\ \frac{\Delta\pi}{\bar{C}} \end{bmatrix} \quad (7)$$

The determinant of matrix $[H]$ can be rewritten as

$$\det[H] = \bar{C} \left[\frac{\omega}{L_p} + \bar{C}(1 - \sigma)^2 \right] \quad (8)$$

By comparing Eqs. (3) and (7) for selective membrane ($L_p > 0, 0 < \sigma < 1$ and $\omega > 0$), we obtain $H_{11} = L_p^{-1}, H_{12} = -(1 - \sigma)\bar{C} \neq H_{21} = \bar{C}(1 - \sigma)$ and $H_{22} = \bar{C}\omega$. This means that in the Eq. (7), the symmetry relation $H_{12} = H_{21}$ is not fulfilled. For unselective membrane ($\sigma = 0$) we can write $H_{11} = (L_p)^{-1}$ and $H_{12} = \bar{C}, H_{22} = \bar{C}\omega$. Additionally, for unselective membrane, the Eq. (7) can be written in a following form $\det[H] = \bar{C}\omega(L_p)^{-1}$. The transport properties of semipermeable membrane are characterized by $L_p > 0, \sigma = 1$ and $\omega = 0$. In that case for this membrane $H_{12} = H_{21} = H_{22} = 0$ and $\det[H] = 0$.

The results of experimental studies for a Nephrophan membrane and aqueous solutions of glucose presented in the previous paper (Ślęzak et al. 2010) suggest that $(\zeta_p)_r = (\zeta_a)_r = 1$ and $(\zeta_v)_r = (\zeta_s)_r = \zeta_r$. In the paper (Ślęzak et al. 2005) it was shown that ζ_r coefficient can be presented in the form

$$\zeta_r = D_r(D_r + 2RT\omega\delta_r)^{-1} \quad (9)$$

where D_r —diffusion coefficient, RT —product of the gas constant and the thermodynamic temperature δ_r —thickness of the concentration boundary layers, $r = A$ or B . Diffusive–convective conditions occur when the concentration exceeds the critical value \bar{C}_{cr} (Ślęzak et al. 2010).

When we divide suitable coefficients of matrixes $[H^*]$ and $[H]$ for diffusive ($r = A$) or convective states ($r = B$) we obtain

$$\frac{(H_{11}^*)_r}{H_{11}} = \frac{(H_{21}^*)_r}{H_{21}} = 1 \tag{10}$$

$$\frac{(H_{12}^*)_r}{H_{12}} = \frac{1 - \zeta_r \sigma}{1 - \sigma} = \frac{2RT\omega\delta_r + D_r(1 - \sigma)}{(1 - \sigma)(D_r + 2RT\omega\delta_r)} \tag{11}$$

$$\frac{(H_{22}^*)_r}{H_{22}} = \zeta_r = \frac{D_r}{D_r + 2RT\omega\delta_r} \tag{12}$$

$$\frac{\det[H^*]_r}{\det[H]} = \det\left(\frac{[H^*]_r}{[H]}\right) = \frac{\zeta_r \omega + \bar{C}L_p(1 - \zeta_r \sigma)(1 - \sigma)}{\omega + \bar{C}L_p(1 - \sigma)^2} \tag{13}$$

Considering the Eq. (9) in Eq. (13) we obtain

$$\frac{\det[H^*]_r}{\det[H]} = \frac{D_r \omega + \bar{C}L_p(1 - \sigma)[D_r(1 - \sigma) + 2RT\omega\delta_r]}{(D_r + 2RT\omega\delta_r)[\omega + \bar{C}L_p(1 - \sigma)^2]} \tag{13a}$$

The above expressions illustrate the dependence of concentration polarization for diffusive conditions ($r = A$) and a diffusive–convective conditions ($r = B$) on a value of $(H_{12}^*)_r/H_{12}$ and $(H_{22}^*)_r/H_{22}$, and $\det [H^*]_r/\det [H]$. Based on Eqs. (10)–(13), we can write

$$\frac{(H_{12}^*)_r}{H_{12}} = \frac{1}{1 - \sigma} \left(1 - \sigma \frac{(H_{22}^*)_r}{H_{22}} \right) \tag{14}$$

$$\frac{\det[H^*]}{\det[H]} = \alpha_1 \left(\alpha_2 + \alpha_3 \frac{(H_{22}^*)_r}{H_{22}} \right) \tag{15}$$

where $\alpha_1 = [\omega + \bar{C}L_p\sigma(1 - \sigma)^2]^{-1}$, $\alpha_2 = \bar{C}L_p(1 - \sigma)$, $\alpha_3 = \omega - \bar{C}L_p\sigma(1 - \sigma)$.

It can be assumed that a value of diffusion coefficient (D_A) under diffusive conditions is constant and independent of \bar{C} . The thickness of concentration boundary layer under diffusive conditions (δ_A and δ_B for $\bar{C} < \bar{C}_{cr}$) is different than under diffusive–convective conditions (δ_B for $\bar{C} \geq \bar{C}_{cr}$) and is dependent on \bar{C} (Ślęzak et al. 2010).

The diffusion coefficient for the convection–diffusion conditions (D_B) is dependent on the concentration of the solutions (Ślęzak et al. 2010). In order to calculate coefficient D_B we transform Eq. (14) into

$$D_B^2 + a_1 D_B + a_2 = 0 \tag{16}$$

where $a_1 = 2RT\omega\delta_B$, $a_2 = -gRT\omega\delta_B^4\alpha_C(C_h - C_l)(R_Cv)^{-1}$.

3 Results and Discussion

In our previous papers (Ślęzak et al. 2012a, b; Batko et al. 2014a, b, 2015) we used the coefficients of concentration polarization ($\zeta_p, \zeta_v, \zeta_s$ and ζ_a) and membrane transport parameters (L_p, σ, ω) to calculate the matrices $[R^*]$, $[L^*]$ and $[P^*]$. The coefficients of concentration polarization and membrane transport parameters are contained in the Kedem–Katchalsky formalism. The procedure used to determine the coefficients $\zeta_p, \zeta_v, \zeta_s$ and ζ_a was also described in the previous paper (Ślęzak et al. 2010). In the present paper we used these coefficients and parameters to calculate the coefficients $H_{11}^*, H_{12}^*, H_{21}^*$ and H_{22}^* in the matrix $[H^*]$. In the previous paper (Ślęzak et al. 2010) we showed that only coefficients $(\zeta_v)_r$

Table 1 Values of the concentration polarization coefficient (ζ_i) and thicknesses of concentration boundary layers (δ_i) in configurations *A* (ζ_A, δ_A) and *B* (ζ_B, δ_B) for mean concentrations of glucose (\bar{C}) (Ślęzak et al. 2010)

	\bar{C} (mol m ⁻³)	ζ_i		$\delta_i \times 10^3$ (m)	
		ζ_A	ζ_B	δ_A	δ_B
	2.7905	0.208	0.208	0.698	0.698
	4.1703	0.208	0.208	0.698	0.698
	5.4101	0.208	0.208	0.698	0.698
	6.5692	0.200	0.209	0.720	0.641
	7.6732	0.190	0.210	0.760	0.576
	8.7362	0.176	0.220	0.810	0.550
	9.7669	0.168	0.260	0.871	0.552
	10.7713	0.155	0.285	0.952	0.600
	11.7535	0.144	0.320	1.046	0.632
	12.7167	0.134	0.348	1.133	0.654
	13.6634	0.126	0.371	1.214	0.669
	14.5954	0.120	0.390	1.291	0.679
	15.5144	0.114	0.406	1.361	0.685
	16.4216	0.110	0.420	1.428	0.688
	17.3180	0.106	0.432	1.490	0.690
	18.2048	0.102	0.442	1.549	0.689
	19.0820	0.100	0.451	1.607	0.688
	19.9518	0.096	0.459	1.664	0.686
	20.8130	0.092	0.467	1.721	0.683
	21.6679	0.088	0.473	1.760	0.677

and $(\zeta_s)_r$ ($r = A, B$) depended on the concentration of solutions and membrane system configuration. The value of $\zeta_p = \zeta_a = 1$ both for solution homogeneity and for concentration polarization, regardless of solution concentration and membrane system configurations (Ślęzak et al. 2010). To calculate H_{12}^* and H_{22}^* , ratios H_{12}^*/H_{12} and H_{22}^*/H_{22} , determinants $\det [H^*]_r$, $\det [H]$ and ratio of the determinants $\det [H^*]_r/\det [H]$, we used the following data (Ślęzak 1989): $L_p = (4.9 \pm 0.1) \times 10^{-12} \text{ m}^3 \text{ N}^{-1} \text{ s}^{-1}$, $\sigma = (6.8 \pm 0.1) \times 10^{-2}$, $\omega = (8.0 \pm 0.3) \times 10^{-10} \text{ mol N}^{-1} \text{ s}^{-1}$, $D_A = D_d = 0.69 \times 10^{-9} \text{ m}^2 \text{ s}^{-1}$, ($T = 295 \pm 0.2$) K, $R = 8.31 \text{ J mol}^{-1} \text{ K}^{-1}$ and values of dependencies $\delta_r = f(\bar{C})$ and $\zeta_r = f(\bar{C})$ ($r = A, B$) presented in Table 1. To calculate the coefficient D_B , we used dependence $\delta_B = f(\bar{C})$ presented in Table 1 and $g = 9.81 \text{ m s}^{-2}$, $\alpha_C = 6.01 \times 10^{-5} \text{ m}^3 \text{ mol}^{-1}$, $\nu = 1.012 \times 10^{-6} \text{ m}^2 \text{ s}^{-1}$.

Calculations based on Eqs. (5) and (7) show that $H_{11}^* = H_{11} = 2 \times 10^{11} \text{ N s m}^{-3}$ are independent of both concentration of solutions and the configuration of the membrane system. Therefore, the values of these coefficients are identical, in condition of both homogeneity and concentration polarization of solutions separated by the membrane ($H_{11}^*/H_{11} = 1$).

Dependencies of coefficients $(H_{12}^*)_r = f(\bar{C})$, $(H_{21}^*)_r = f(\bar{C})$ and $(H_{22}^*)_r = f(\bar{C})$ on the average concentration \bar{C} and configuration of the membrane system are shown in Figs. 2, 3 and 4. Figure 2 shows that values of coefficients H_{12} , $(H_{12}^*)_A$ and $(H_{12}^*)_B$ decrease almost linearly with the increase in average concentration \bar{C} and these coefficients fulfill the following condition $H_{12} > (H_{12}^*)_B > (H_{12}^*)_A < 0$. Only for $\bar{C} \leq 5.41 \text{ mol m}^{-3}$ $(H_{12}^*)_B = (H_{12}^*)_A$. For coefficient $(H_{12}^*)_r$ and $\bar{C} > 5.41 \text{ mol m}^{-3}$, the difference $\Delta H_{12} = (H_{12}^*)_B - (H_{12}^*)_A < 0$ is a measure of natural convection effect. This expression can also be written as $\Delta H_{12}^* = \bar{C} \sigma (\zeta_B -$

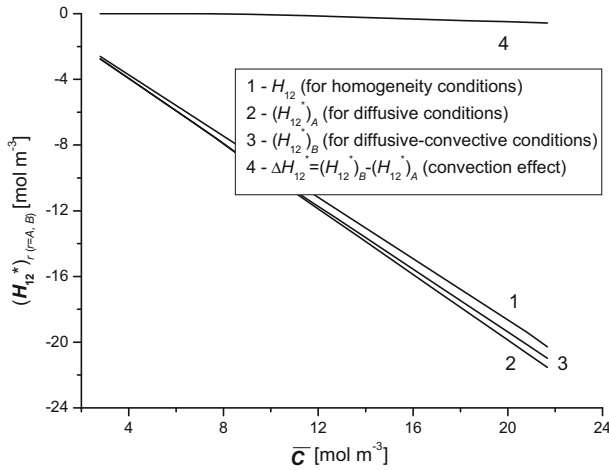


Fig. 2 Graphic illustration of dependences $H_{12} = f(\bar{C})$ (graph 1), $(H_{12}^*)_A = f(\bar{C})$ (graph 2) and $(H_{12}^*)_B = f(\bar{C})$ (graph 3) calculated based on Eq. (5) for aqueous glucose solutions in an homogeneity solution conditions (graph 1), diffusive condition (graph 2) and diffusive–convective condition (graph 3). Line 4 represents the dependence $\Delta H_{12}^* = (H_{12}^*)_B - (H_{12}^*)_A = f(\bar{C})$ for convection effect

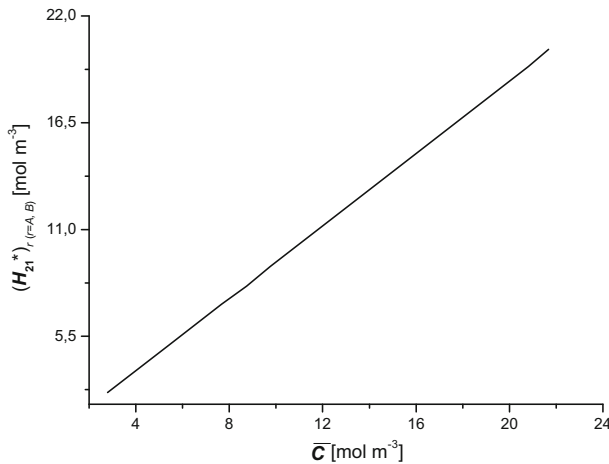


Fig. 3 Graphic illustration of dependence $(H_{21}^*)_{r(r=A,B)} = H_{21} = f(\bar{C})$ calculated based on Eq. (5) for aqueous glucose solutions in concentration polarization conditions and homogeneity solution conditions

ζ_A). Figure 3 shows that values of coefficients H_{21} and $(H_{21}^*)_r$ increase linearly with increase of \bar{C} and that $H_{21} = (H_{21}^*)_r > 0$. This indicates that the values of these coefficients are independent of the membrane system configuration or conditions under which they were applied, i.e., $(H_{21}^*)_r/H_{21} = 1$.

Graph 1 in Fig. 4 shows that dependence $(H_{22}^*)_r = f(\bar{C})$ obtained for the conditions of homogeneity of solutions separated by the membrane is linear. Dependence $(H_{22}^*)_A = f(\bar{C})$ obtained for diffusive conditions (curve 2) and dependence $(H_{22}^*)_B = f(\bar{C})$ obtained for diffusive–convective conditions (curve 3) show that the coefficients $(H_{22}^*)_A$ and $(H_{22}^*)_B$ are nonlinearly dependent on the average concentration \bar{C} and fulfill the condition $(H_{22}^*)_A <$

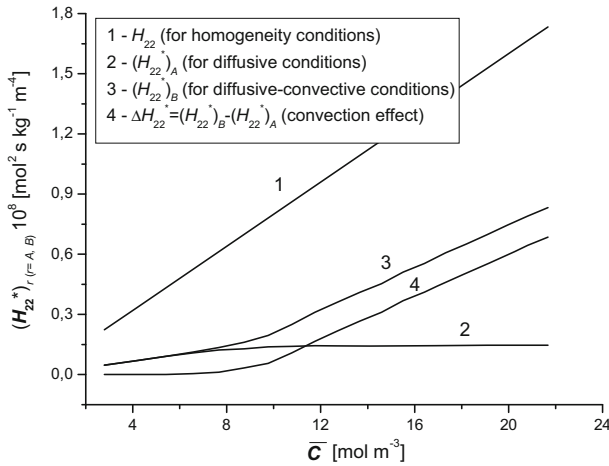


Fig. 4 Graphic illustration of dependence $H_{22} = f(\bar{C})$ (line 1), $(H_{22}^*)_A = f(\bar{C})$ (curve 2), $(H_{22}^*)_B = f(\bar{C})$ (curve 3) calculated based on Eq. (5) for aqueous glucose solutions in a homogeneity solution conditions (line 1), diffusive condition (curve 2) and diffusive–convective condition (curve 3). Curve 4 represents the dependence $\Delta H_{22}^* = (H_{22}^*)_B - (H_{22}^*)_A = f(\bar{C})$ for convection effect

$(H_{22}^*)_B < H_{22}$. For $\bar{C} \leq 5.41 \text{ mol m}^{-3}$, $(H_{22}^*)_A = (H_{22}^*)_B$ and for $\bar{C} > 5.41 \text{ mol m}^{-3}$, $(H_{22}^*)_B > (H_{22}^*)_A$. The difference $\Delta H_{22}^* = (H_{22}^*)_B - (H_{22}^*)_A$ is a measure of natural convection effect for coefficient H_{22}^* . For graph 4 presented in Fig. 4 we obtain: $\Delta H_{22}^* = 0$ (for $\bar{C} \leq 5.41 \text{ mol m}^{-3}$) and $\Delta H_{22}^* > 0$ (for $\bar{C} > 5.41 \text{ mol m}^{-3}$). The expression for ΔH_{22}^* can also be written in the following form $\Delta H_{22}^* = \bar{C}\omega(\zeta_B - \zeta_A)$.

In Fig. 5 different versions of dependence $\det[H^*]_r = f(\bar{C})$ are presented. For the solution homogeneity conditions, this dependence can be described as $\det[H] = f(\bar{C})$ illustrated in graph 1. Graph 2 obtained for diffusive conditions illustrates the dependence $\det[H^*]_A = f(\bar{C})$, and graph 3 obtained for the diffusive–convective conditions illustrates dependence $\det[H^*]_B = f(\bar{C})$. Comparison of graphs 2 and 3 results in $\det[H^*]_B = \det[H^*]_A$ (for $\bar{C} \leq 5.41 \text{ mol m}^{-3}$) and $\det[H^*]_B > \det[H^*]_A$ (for $\bar{C} > 5.41 \text{ mol m}^{-3}$). Furthermore, the difference $\Delta(\det[H^*]) = \det[H^*]_B - \det[H^*]_A = \bar{C}(\zeta_B - \zeta_A)[\omega L_p^{-1} - \bar{C}\sigma(1 - \sigma)]$ defines the natural convection effect for $\det[H_{22}^*]_r$ (curve 4).

Figure 6 shows a dependence $D_B = f(\bar{C})$ obtained from solution of Eq. (16). From the curve shown in this figure it results that for $6.57 \text{ mol m}^{-3} < \bar{C} \leq 9.32 \text{ mol m}^{-3}$, the value $D_B < D_A$ and that for $\bar{C} > 9.32 \text{ mol m}^{-3}$ D_B increases linearly with the increase of \bar{C} . In configuration B for $\bar{C} \geq \bar{C}_r$, $D_B = D_d + D_{dk}$ and $D_{dk} > D_d$. Therefore, $D_{dk}/D_d = D_B/D_A - 1$. It can be shown that for $\bar{C} > 9.32 \text{ mol m}^{-3}$ $D_{dk}/D_d > 0$ and increases with the increase of \bar{C} and for $\bar{C} = 21.67$, $D_{dk}/D_d = 2.84$.

Figure 7 is a graphical illustration of dependence $(H_{12}^*)_r/H_{12} = f(\bar{C})$ for the conditions of diffusion (curves 1 and 1') and a diffusion–convection (curves 2 and 2'). Curve 1 presents the solution of Eq. (11), and the curve 1' presents solution of Eq. (11) considering the Eq. (9). The curves 2 and 2' illustrate the results of calculations carried out based on Eq. (11) considering the Eq. (9) and results of calculations $D_B = f(\bar{C})$ performed based on Eq. (16). The course of the curves presented in the Fig. 7 shows that for $\bar{C} \leq 5.41 \text{ mol m}^{-3}$ $(H_{12}^*)_A/H_{12} = (H_{12}^*)_B/H_{12} = 1.06$ and for the $\bar{C} > 5.41 \text{ mol m}^{-3}$ $(H_{12}^*)_A/H_{12} > (H_{12}^*)_B/H_{12}$.

Figure 8 is a graphical illustration of dependence $(H_{22}^*)_r/H_{22} = f(\bar{C})$ for the conditions of diffusion (curves 1 and 1') and a diffusion–convection (curves 2 and 2').

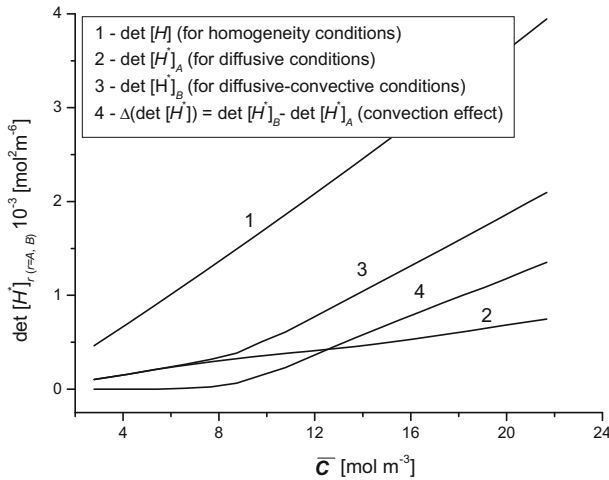


Fig. 5 Graphic illustration of dependence $\det [H] = f(\bar{C})$ (line 1), $\det [H^*]_A = f(\bar{C})$ (curve 2) and $\det [H^*]_B = f(\bar{C})$ (curve 3) calculated based on Eq. (6) for aqueous glucose solutions in homogeneity solution conditions (line 1) and concentration polarization conditions: diffusive condition (curve 2) and diffusive-convective condition (curve 3). Curve 4 represents the dependence $\Delta(\det [H^*]) = \det [H^*]_B - \det [H^*]_A = f(\bar{C})$ for convection effect

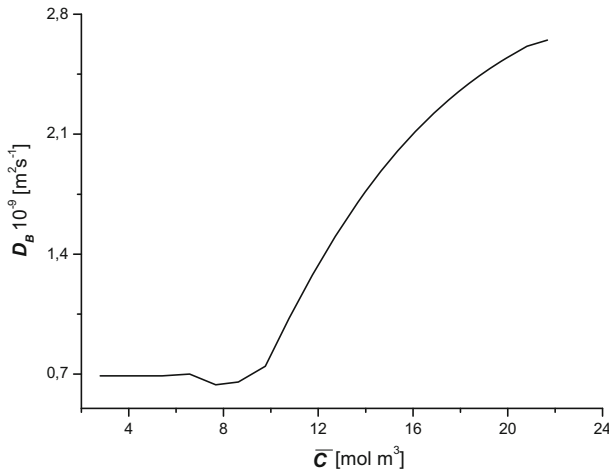


Fig. 6 Graphic illustration of dependence $D_B = f(\bar{C})$ calculated based on Eq. (15) for aqueous glucose solutions in configuration B of a single-membrane system (diffusive-convective condition)

Curve 1 shows the results of calculations performed based on Eq. (13) and the curve 1' based on Eq. (13) considering the Eq. (9). Curves 2 and 2' illustrate the results of calculations performed based on Eqs. (13) and (9) considering the results of calculations $D_B = f(\bar{C})$ performed based on Eq. (16). The course of the curves presented in Fig. 8 indicates that for $\bar{C} \leq 5.41 \text{ mol m}^{-3} (H_{22}^*)_A/H_{22} = (H_{22}^*)_B/H_{22} = 0.21$ and for $\bar{C} > 5.41 \text{ mol m}^{-3} (H_{22}^*)_B/H_{22} > (H_{22}^*)_A/H_{22}$.

Figure 9 shows graphical dependencies $\det [H^*]_r/\det [H] = f(\bar{C})$ for the diffusive conditions (curves 1 and 1') and the diffusive-convective conditions (curves 2 and 2').

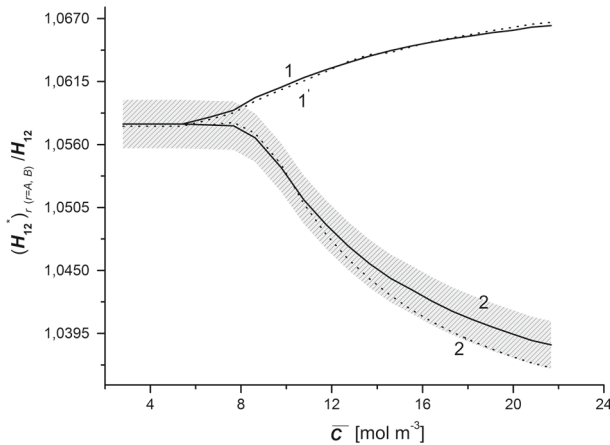


Fig. 7 Graphic illustration of dependence $(H_{12}^*)_A/H_{12} = f(\bar{C})$ (curves 1, 1') (curves 1 and 1') and $(H_{12}^*)_B/H_{12} = f(\bar{C})$ (curves 2 and 2') for the configuration A and B of the membrane system, respectively. Curves 1 and 2 were calculated based on Eq. (11), whereas curves 1' and 2' based on Eqs. (11) and (15). The courses of curves 2 and 2' are located within 0.2% error range

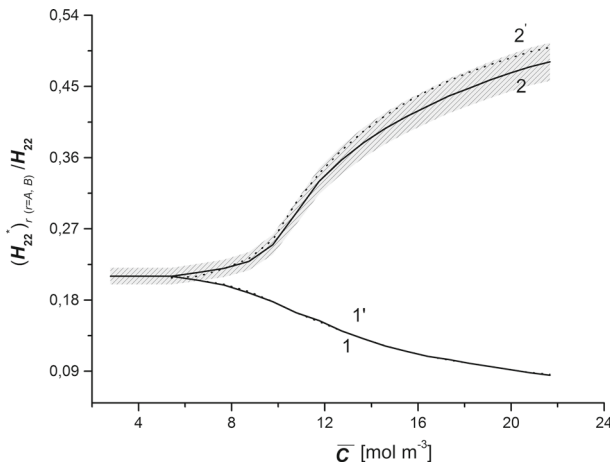


Fig. 8 Graphic illustration of dependence $(H_{22}^*)_A/H_{22} = f(\bar{C})$ (graph 1 and 1') and $(H_{22}^*)_B/H_{22} = f(\bar{C})$ (graph 2 and 2') for the configuration A and B of the membrane system, respectively. Curves 1 and 2 were calculated based on Eq. (13), whereas curves 1' and 2' based on Eqs. (13) and (15). The courses of curves 2 and 2' are located within the 5% error range

Curve 1 and curve 1' represent the results of calculations performed based on Eqs. (13) and (13a), respectively. The curves 2 and 2' illustrate the results of calculations performed based on Eqs. (13) and (13a), considering the results of calculations $D_B = f(\bar{C})$ that were based on Eq. (16). The courses of the curves presented in the figure show that for $\bar{C} \leq 5.41 \text{ mol m}^{-3} \det [H^*]_A / \det [H] = \det [H^*]_B / \det [H] = 0.23$ and for the $\bar{C} > 5.41 \text{ mol m}^{-3} \det [H^*]_B / \det [H] > \det [H^*]_A / \det [H]$.

Similar to pairs of coefficients L_{ij} and L_{ij}^* , R_{ij} and R_{ij}^* , P_{ij} and P_{ij}^* , ($i, j \in \{1, 2\}$) with the same indices, for pair of Peusner's coefficients H_{ij} and H_{ij}^* , units are the same and values are different. Comparing diagonal and non-diagonal coefficients of matrix $[H^*]$

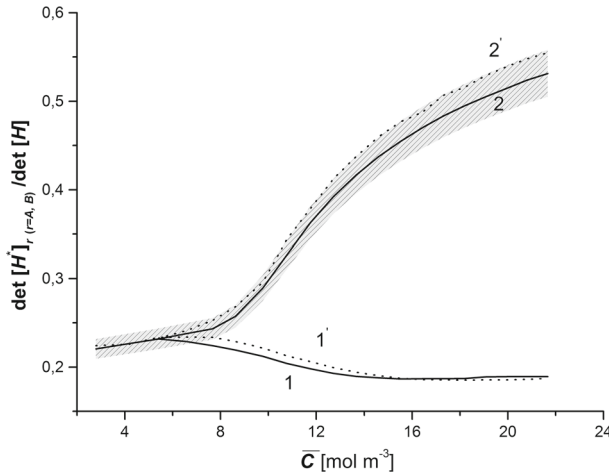


Fig. 9 Graphic illustration of dependences $\det \{[H^*]_A/[H]\} = f(\bar{C})$ (curves 1 and 1') and $\det \{[H^*]_B/[H]\}$ (curves 2 and 2') for the configuration A and B of the membrane system, respectively. Curves 1 and 2 were calculated based on Eq. (14), whereas curves 1' and 2' based on Eqs. (14) and (15). The courses of curves 2 and 2' are located within the 5% error range

with different indices, units are different and values differ by over tenfold. Similarly to L_{ij}^*/L_{ij} , R_{ij}^*/R_{ij} and P_{ij}^*/P_{ij} ratios, H_{ij}^*/H_{ij} , ratio is dimensionless and its values have the same order of magnitude at least for a Nephrophan membrane and water glucose solutions. This facilitates analysis of the results obtained under conditions of concentration polarization or homogeneity of solutions. Calculation of $\det [H^*]/[H]$ allows to reduce the number of Peusner's coefficients needed to characterize transport properties of the membrane.

Considering the Eqs. (10)–(13) and the results obtained in previous papers (Ślęzak et al. 2012a, b; Batko et al. 2014a, b, 2015) we can write

$$\frac{(H_{11}^*)_r}{H_{11}} = \frac{(L_{11}^*)_r}{L_{11}} = \frac{(H_{21}^*)_r}{H_{21}} = \frac{(L_{21}^*)_r}{L_{21}} = 1 \tag{17}$$

$$\frac{(H_{12}^*)_r}{H_{12}} = \frac{(L_{12}^*)_r}{L_{12}} = \zeta_r \frac{(R_{12}^*)_r}{R_{12}} = \frac{[\zeta_r \omega + \beta_1(1 - \zeta_r \sigma)]}{L_p \beta_2} \frac{(P_{12}^*)_r}{P_{12}} \tag{18}$$

$$\frac{(H_{22}^*)_r}{H_{22}} = \frac{R_{22}}{(R_{22}^*)_r} = \beta_3 \left(\beta_2 \frac{(L_{22}^*)_r}{L_{22}} - \beta_1 \right) = \beta_3 \left(\beta_2 \frac{P_{22}}{(P_{22}^*)_r} - \beta_1 \right) \tag{19}$$

$$\det \left(\frac{[H^*]}{[H]} \right) = \det \left(\frac{[P]}{[P^*]} \right) = \beta_2 \left[\beta_1 + \beta_3 \det \left(\frac{[L^*]}{[L]} \right) \right] = \beta_2 \left[\beta_1 + \beta_3 \det \left(\frac{[R^*]}{[R]} \right) \right] \tag{20}$$

where $\beta_1 = \bar{C}L_p(1 - \sigma)$, $\beta_2 = \omega + \bar{C}L_p(1 - \sigma)^2$, $\beta_3 = [\omega - \bar{C}L_p\sigma(1 - \sigma)]^{-1}$.

To show the dependence between the configurations B and A of the membrane system we calculate the respective quotients of coefficients $H_{11}^*, H_{12}^*, H_{21}^*, H_{22}^*$ and $\det [H^*]$ for configurations B and A of the membrane system following the expressions written below:

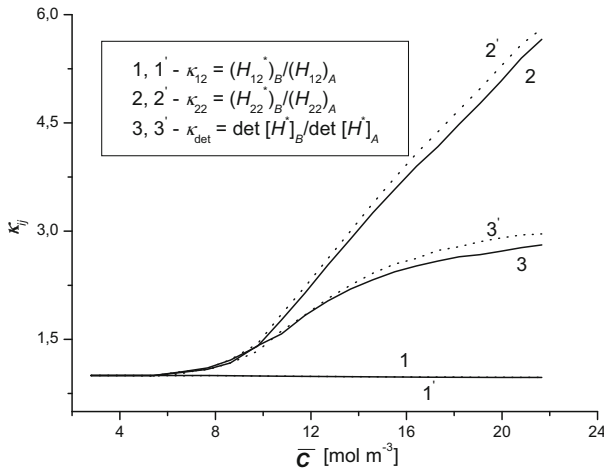


Fig. 10 Graphic illustration of dependencies $\kappa_{12} = (H_{12}^*)_B / (H_{12}^*)_A = f(\bar{C})$ (curves 1, 1'), $\kappa_{22} = (H_{22}^*)_B / (H_{22}^*)_A = f(\bar{C})$ (curves 2, 2') and $\kappa_{\text{det}} = \det [H^*]_B / \det [H^*]_A$ (curves 3 and 3'), respectively. Curves 1 and 2 were calculated based on Eq. (17), curve 3 based on Eq. (18) and curves 1'–3' based on Eqs. (19)–(21), respectively

$$\kappa_{ij} = \frac{(H_{ij}^*)_B}{(H_{ij}^*)_A}, \quad i, j = 1, 2 \tag{21}$$

$$\kappa_{\text{det}} = \frac{\det[H^*]_B}{\det[H^*]_A} \tag{22}$$

Considering above equations, Eqs. (5) and (9) with the use of relatively simple algebraic operation, we obtain

$$\kappa_{12} = \frac{(H_{12}^*)_B}{(H_{12}^*)_A} = \frac{1 - \zeta_B(\bar{C})}{1 - \zeta_A(\bar{C})} \tag{23}$$

$$\kappa_{22} = \frac{(H_{22}^*)_B}{(H_{22}^*)_A} = \frac{\zeta_B(\bar{C})}{\zeta_A(\bar{C})} = \frac{1 - \kappa_{12}[1 - \zeta_A(\bar{C})]}{\zeta_A(\bar{C})} \tag{24}$$

$$\kappa_{\text{det}} = \frac{\zeta_B(\bar{C})\omega + \bar{C}L_p[1 - \zeta_B(\bar{C})\sigma](1 - \sigma)}{\zeta_A(\bar{C})\omega + \bar{C}L_p[(1 - \zeta_A(\bar{C})\sigma)(1 - \sigma)]} \tag{25}$$

where $\zeta_B(\bar{C}) = D_B(\bar{C})[D_B(\bar{C}) + 2RT\omega\delta_B(\bar{C})]^{-1}$, $\zeta_A(\bar{C}) = D_A(\bar{C})[D_A(\bar{C}) + 2RT\omega\delta_A(\bar{C})]^{-1}$.

Calculations show that $\kappa_{11} = \kappa_{12} = 1$. In Fig. 10 curves 1, 1', 2, 2', 3 and 3' illustrate the dependence $\kappa_{12} = f(\bar{C})$, $\kappa_{22} = f(\bar{C})$ and $\kappa_{\text{det}} = f(\bar{C})$ calculated on the basis of Eqs. (23)–(25), considering the dependence $D_B = f(\bar{C})$ shown in Fig. 6 and $\delta_A = f(\bar{C})$ and $\delta_B = f(\bar{C})$ shown in Table 1.

From the Fig. 10 it results that coefficients κ_{12} , κ_{22} and κ_{det} do not depend on the concentration of solutions separated by a membrane and membrane system configurations $\bar{C} \leq 5.41 \text{ mol m}^{-3}$. For this range of concentration their values are $\kappa_{12} = \kappa_{22} = \kappa_{\text{det}} = 1$, similar to a value of the last common point of the curves 1, 2, 3 and 4. Similarly to the curves shown in the previous figures, the last common point with coordinates $\bar{C} = 5.41 \text{ mol m}^{-3}$

and $\kappa_{12} = \kappa_{22} = \kappa_{\text{det}} = 1$ may be considered as a bifurcation point. Only for $\bar{C} > 5.41 \text{ mol m}^{-3}$, κ_{12} values are independent of the concentration of solutions separated by a membrane with accuracy to the second significant digit. A comparison of these characteristics shows that for the same value of \bar{C} condition $\kappa_{22} > \kappa_{\text{det}} > \kappa_{12}$ is satisfied.

To show the dependence between the states of diffusion–convection, diffusion and homogeneity, we define the coefficients χ_{12} , χ_{22} and χ_{det}

$$\chi_{12} = \frac{(H_{12}^*)_B - (H_{12}^*)_A}{H_{12}} = -\frac{\sigma}{1 - \sigma} [\zeta_B(\bar{C}) - \zeta_A(\bar{C})] \tag{26}$$

$$\chi_{22} = \frac{(H_{22}^*)_B - (H_{22}^*)_A}{H_{22}} = \zeta_B(\bar{C}) - \zeta_A(\bar{C}) \tag{27}$$

$$\chi_{\text{det}} = \frac{\det[H^*]_B - \det[H^*]_A}{\det[H]} = \frac{[\zeta_B(\bar{C}) - \zeta_A(\bar{C})][\omega - \bar{C}L_p\sigma(1 - \sigma)]}{\omega + \bar{C}L_p(1 - \sigma)^2} \tag{28}$$

where $\zeta_B(\bar{C}) = D_B(\bar{C})[D_B(\bar{C}) + 2RT\omega\delta_B(\bar{C})]^{-1}$, $\zeta_A(\bar{C}) = D_A(\bar{C})[D_A(\bar{C}) + 2RT\omega\delta_A(\bar{C})]^{-1}$.

In Fig. 11, curves 1, 1', 2, 2', 3 and 3' illustrate the dependence $\chi_{12} = f(\bar{C})$, $\chi_{22} = f(\bar{C})$ and $\chi_{\text{det}} = f(\bar{C})$ calculated based on Eqs. (26)–(28) considering dependences $D_B = f(\bar{C})$ shown in Fig. 6 and dependence $\delta_A = f(\bar{C})$ and $\delta_B = f(\bar{C})$ shown in Table 1. The results of calculations are shown in Figs. 2, 3, 4 and 5. The courses of the curves presented in this figure show that for $\bar{C} \leq 5.41 \text{ mol m}^{-3}$ the relation $\chi_{12} = \chi_{22} = \chi_{\text{det}} = 0$ is satisfied. For $\bar{C} > 5.41 \text{ mol m}^{-3}$ dependences $\chi_{22} > \chi_{\text{det}} > \chi_{12}$, $\chi_{12} < 0$, $0 < \chi_{22} < 0.5$ and $0 < \chi_{\text{det}} < 0.5$ are fulfilled. Moreover, this figure shows that curves 1 and 1' nearly overlap and the curves 2 and 2' and 3 and 3' are located within the 5% error range. Moreover, curves 2, 2', 3 and 3' are located within the 15% error range. Comparing Eqs. (26)–(28) it may be noticed that

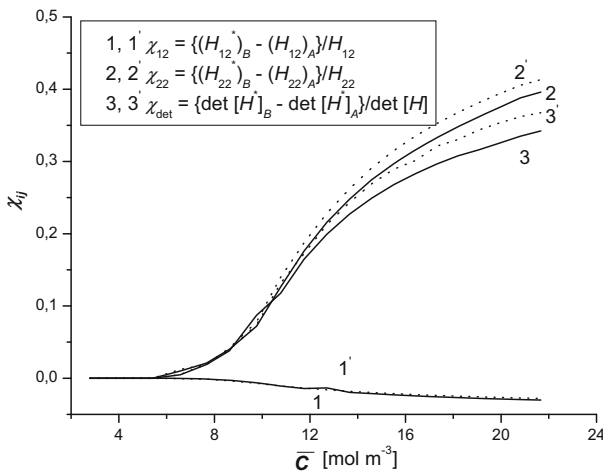


Fig. 11 Graphic illustration of dependences $\chi_{12} = \{(H_{12}^*)_B - (H_{12}^*)_A\}/H_{12} = f(\bar{C})$ (curve 1, 1'), $\chi_{22} = \{(H_{22}^*)_B - (H_{22}^*)_A\}/H_{22} = f(\bar{C})$ (curve 2, 2') and $\chi_{\text{det}} = \{\det[H^*]_B - \det[H^*]_A\}/\det[H] = f(\bar{C})$ (curve 3, 3'). Curves 1–3 and 1'–3' were calculated based on Eqs. (22)–(24), respectively

$$\chi_{12} = -\frac{\sigma}{1-\sigma}\chi_{22} \tag{29}$$

$$\chi_{\text{det}} = \frac{\omega - \bar{C}L_p\sigma(1-\sigma)}{\omega + \bar{C}L_p(1-\sigma)^2}\chi_{22} \tag{30}$$

The values of $(H_{ij}^*)_r$ ($r = A$ or B) were compared to the values of coefficients H_{ij} (for homogeneity solution conditions). Calculations show that $H_{11} = H_{11}^* = \text{const}$. For $\bar{C} > 5.41 \text{ mol m}^{-3}$ condition $(H_{12}^*)_A < (H_{12}^*)_B < H_{12} < 0$ is fulfilled and the coefficients $(H_{12}^*)_B, (H_{12}^*)_A$, and H_{12} are approximately linearly dependent on \bar{C} . Values of the coefficient $H_{21} = H_{21}^*$ are positive and linearly dependent on \bar{C} . For $\bar{C} > 5.41 \text{ mol m}^{-3}$ condition $(H_{22}^*)_A < (H_{22}^*)_B < H_{22} > 0$ is fulfilled and the coefficients $(H_{22}^*)_A, (H_{22}^*)_B, H_{22}$, and H_{12} are nonlinearly dependent on \bar{C} and dependent on the membrane system configuration. In addition, coefficients that facilitate interpretation of the calculations results are defined using various differences and ratios of coefficients $(H_{ij}^*)_r$ and H_{ij} , with the same indicators for the A and B configurations of the membrane system. It is also shown that there is a threshold value of \bar{C} , above which the ratios $(H_{12}^*)_r/H_{12}$ and $(H_{22}^*)_r/H_{22}$ are dependent both on \bar{C} and the configuration of the membrane system.

The evolution of thermodynamic systems can be described using dependences $\varphi = f(\lambda)$, where φ is the order parameter and λ is the critical parameter (Kondepudi 2008). In the case investigated in the paper, the concentration \bar{C} may be a control parameter that may be used to determine distance of the system from equilibrium. If \bar{C} increases, the system recedes from equilibrium and in the point where $\bar{C} = \bar{C}_{\text{cr}}$ reaches the threshold of thermodynamic branch stability at the bifurcation point. At or near the equilibrium state ($\bar{C} = 0$) (in the configuration A and in configuration B for $\bar{C} < \bar{C}_{\text{cr}}$) steady state is gravitationally stable, since the influence of the gravitational field on the membrane transport is negligible. Starting at this point, the thermodynamic branch becomes unstable due to concentration (density) fluctuations and the increasing difference in concentrations causes a stationary non-equilibrium state, to which the system heads spontaneously. This state may be more complex than the corresponding equilibrium state. Dworecki et al. (1995, 2005), used laser interferometry to show that interference fringes are regular and its curvature is present only in the CBL areas in this condition. If we gradually increase value \bar{C} for $\bar{C} > \bar{C}_{\text{cr}}$, then in the non-equilibrium state the layer system loses stability as evidenced by convection flows. Therefore, interference fringes are irregular (Dworecki et al. 2005). This means that in the absence of the gravitational field ($g = 0$) or under conditions where the two solutions separated by a membrane are homogeneous solutions (thoroughly mixed by mechanical stirrers serve as idealization of this state) configurations A and B of membrane system are equivalent. In contrast, the CBL system is not sensitive to change in the direction of constant gravitational field after changing from A to B configuration (in concentration range $\bar{C} < \bar{C}_{\text{cr}}$), and then the CBL system is equally probable. Consideration of the influence of the gravitational field ($g \neq 0$) changes the bifurcation diagram from symmetrical to asymmetrical (Kondepudi and Prigogine 1981). From interferometric research it results that in the concentrations range $\bar{C} > \bar{C}_{\text{cr}}$, CBL system in configuration B is sensitive to the influence of constant gravitational field. In conditions that are distant from equilibrium and for membrane with regular, square pores, solutions located above and below the membrane form dendritic spatial structure called “plum structure” for the concentration Rayleigh number that is in the following range ($10^{10} \leq R_C \leq 10^{11}$) (Puthenveetil and Arakeri 2008). This “plum structure” can be considered as a dissipative structure, since it is formed under conditions far from equilibrium. This suggests that the role of the order parameter could be played by coefficients $\kappa_{12}, \kappa_{22}, \kappa_{\text{det}}, \chi_{12}, \chi_{22}$ and χ_{det} .

Peusner's Network Thermodynamics (PNT) allows transformation of a symmetric or hybrid membrane transport equations for homogeneous and non-homogeneous binary non-electrolyte solutions. Peusner's procedure enables the transformation of classical Kedem–Katchalsky equations to alternative forms L , R , P or H (for homogeneous solutions), and L^* , R^* , P^* or H^* (for non-homogeneous solutions) of Kedem–Katchalsky equations, by replacing ΔP on $\Delta P - \Delta\pi$ and $\Delta\pi$ on $\Delta\pi/\bar{C} = RT \ln(C_h/C_l)$.

For L , R , P and H Kedem–Katchalsky equations, these transformations provide network forms of these equations with new types of coefficients: L_{ij} , R_{ij} , P_{ij} or H_{ij} ($i, j \in \{1, 2\}$). Each coefficient can be a combination of practical coefficients, i.e., the hydraulic permeability (L_p), the solute permeability (ω) and the reflection (σ) coefficients, and average concentration (\bar{C}), occurring in the classical Kedem–Katchalsky equations. For Nephrophan membrane it can be assumed that coefficients L_p , σ and ω are constant (Ślęzak 1989).

Similarly, for L^* , R^* , P^* and H^* Kedem–Katchalsky equations, these transformations provide network forms of these equations with new types of coefficients: L_{ij}^* , R_{ij}^* , P_{ij}^* or H_{ij}^* ($i, j \in \{1, 2\}$). Each coefficient can be a combination of practical coefficients, i.e., the hydraulic permeability (L_p), the solute permeability (ω) and the reflection (σ) coefficients, average concentration (\bar{C}) and Katchalsky's coefficients: hydraulic (ζ_p), osmotic (ζ_v), advective (ζ_a) and diffusive (ζ_s) occurring in the classical Kedem–Katchalsky equations. The coefficients L_{ij}^* , R_{ij}^* , P_{ij}^* or H_{ij}^* ($i, j \in \{1, 2\}$) may be calculated based on the experimentally determined coefficients L_p , σ , ω , ζ_p , ζ_v , ζ_a and ζ_s . The results of calculations presented in current and previous papers (Ślęzak et al. 2012a, b; Batko et al. 2014a, b, 2015) show that the values of coefficients R_{ij}^* , L_{ij}^* , P_{ij}^* and H_{ij}^* ($i, j \in \{1, 2\}$) are sensitive to the concentration of the solutions separated by a membrane and the order of arrangement of solutions relative to the direction of gravity acceleration. The network forms of K–K equations containing Peusner's coefficients R_{ij}^* , L_{ij}^* , P_{ij}^* and H_{ij}^* ($i, j \in \{1, 2\}$) may be used as a new tool to study membrane transport.

4 Conclusions

1. The paper presents a hybrid matrix form of Kedem–Katchalsky equations that contain coefficients H_{ij}^* ($i, j = 1, 2$) for the conditions of concentration polarization. The obtained equations were applied to the interpretation of transport of the aqueous glucose solutions with concentrations C_h and C_l ($C_h > C_l$) through the Nephrophan membrane that was oriented in the horizontal plane. The calculations of coefficients H_{ij}^* were made for the A and B configurations of the membrane system. In the A configuration glucose solution with concentration C_h was located below the membrane and the solution with concentration C_l above the membrane. In configuration B locations of the solutions were reversed. The values of $(H_{ij}^*)_r$ ($r = A$ or B) were compared to the values of coefficients H_{ij} (for homogeneity solution conditions). Calculations show that $H_{11} = H_{11}^* = \text{const}$.
2. Based on the presented study, we can conclude that PNT is an alternative manner of description of membrane transport both for homogeneity of solutions separated by a membrane and in conditions of concentration polarization.
3. There is a threshold value of concentration \bar{C} , above which the values of coefficients H_{12}^* and H_{22}^* are dependent on the configuration of the membrane system and the values of these coefficients in the convective state are greater than their values in non-convective state.

4. Coefficient H_{11}^* has constant values, i.e., independent of the concentration of solutions separated by a membrane and the membrane system configurations. The coefficients H_{12}^* , H_{21}^* and H_{22}^* are linearly (H_{21}^*) or nonlinearly (H_{12}^* , H_{22}^*) dependent on the solution concentration. For $\bar{C} > 5.41 \text{ mol m}^{-3}$ condition $(H_{12}^*)_B < (H_{12}^*)_A < H_{12} < 0$ is fulfilled and the coefficients $(H_{12}^*)_B$, $(H_{12}^*)_A$, and H_{12} are approximately linearly dependent on \bar{C} . Values of the coefficient $H_{21} = H_{21}^*$ are positive and linearly dependent on \bar{C} . For $\bar{C} > 5.41 \text{ mol m}^{-3}$ condition $(H_{22}^*)_A < (H_{22}^*)_B < H_{22} > 0$ is fulfilled and the coefficients $(H_{22}^*)_A$, $(H_{22}^*)_B$, H_{22} , and H_{12} are nonlinearly dependent on \bar{C} and dependent on the membrane system configuration.
5. Nonlinearity of characteristics $H_{12}^* = f(\bar{C})$ and $H_{22}^* = f(\bar{C})$ is a result of competition between spontaneously occurring processes of diffusion and natural convection.

Open Access This article is distributed under the terms of the Creative Commons Attribution 4.0 International License (<http://creativecommons.org/licenses/by/4.0/>), which permits unrestricted use, distribution, and reproduction in any medium, provided you give appropriate credit to the original author(s) and the source, provide a link to the Creative Commons license, and indicate if changes were made.

References

- Abu-Rjal, R., Chinaryan, V., Rubinstein, I., Zaltzman, B.: Effect of concentration polarization on permselectivity. *Phys. Rev. E* **89**, 012302 (2014)
- Baranowski, B., Kawczyński, A.: Experimental determination of the critical Rayleigh number in electrolyte solutions with concentration polarization. *Electrochim. Acta* **17**, 695–699 (1972)
- Baranowski, B.: The electrochemical analogon of the Benard Instability studied at isothermal and potentiostatic conditions. *J. Non-Equilib. Thermodyn.* **5**, 67–72 (1980)
- Barry, P.H., Diamond, J.M.: Effects of unstirred layers on membrane phenomena. *Physiol. Rev.* **64**, 763–872 (1984)
- Batko, K., Ślęzak-Prochazka, I., Grzegorzczyn, S., Ślęzak, A.: Membrane transport in concentration polarization conditions: network thermodynamics model equations. *J. Porous Media* **17**, 573–586 (2014)
- Batko, K., Ślęzak-Prochazka, I., Ślęzak, A.: Network hybrid form of the Kedem–Katchalsky equations for non-homogenous binary non-electrolyte solutions: evaluation of P_{ij}^* Peusner's tensor coefficients. *Transp. Porous Media* **106**, 1–20 (2015)
- Batko, K., Ślęzak-Prochazka, I., Ślęzak, A.: Network form of the Kedem–Katchalsky equations for ternary non-electrolyte solutions. Part 1–6. *Polim. Med.* **43**, 93–102, 103–109, 111–118, 241–256, 257–275, 277–295 (2013)
- Batko, K., Ślęzak-Prochazka, I., Ślęzak, A.: Network form of the Kedem–Katchalsky equations for ternary non-electrolyte solutions. Part 7, 8. *Polim. Med.* **44**(39–49), 89–107 (2014)
- Demirel, Y.: *Nonequilibrium Thermodynamics: Transport and Rate Processes in Physical, Chemical and Biological Systems*. Elsevier, Amsterdam (2007)
- Dworecki, K.: Interferometric investigations of near-membrane diffusion layers. *J. Biol. Phys.* **21**, 37–49 (1995)
- Dworecki, K., Wąsik, S., Ślęzak, A.: Temporal and spatial structure of the concentration boundary layers in a membrane system. *Phys. A* **326**, 360–369 (2003)
- Dworecki, K., Ślęzak, A., Ornal-Wąsik, B., Wąsik, S.: Effect of hydrodynamic instabilities on solute transport in a membrane system. *J. Membr. Sci.* **265**, 94–100 (2005)
- Fernández-Sempere, J., Ruiz-Beviá, F., Garcia-Algado, P., Salcedo-Díaz, R.: Visualization and modeling of the polarization layer and reversible adsorption process in PEG-10000 dead-end ultrafiltration. *J. Membr. Sci.* **342**, 279–290 (2009)
- Grzegorzczyn, S., Jasik-Ślęzak, J., Michalska-Małecka, K., Ślęzak, A.: Transport of non-electrolyte solutions through membrane with concentration polarization. *Gen. Physiol. Biophys.* **27**, 315–321 (2008)
- Grzegorzczyn, S., Ślęzak, A.: Conditions of hydrodynamic instability appearance in fluid thin layers with changes in time thickness and density gradient. *J. Non-Equilib. Thermodyn.* **37**, 77–98 (2012)
- Han, Y., Grier, D.G.: Colloidal electroconvection in a thin horizontal cell: I. Microscopic cooperative patterns at low voltage. *J. Chem. Phys.* **122**, 164701 (2005)

- Han, Y., Grier, D.G.: Colloidal electroconvection in a thin horizontal cell: II. Bulk electroconvection of water during parallel-plate electrolyte. *J. Chem. Phys.* **125**, 144707 (2006)
- Han, Y., Grier, D.G.: Colloidal electroconvection in a thin horizontal cell: III. Interfacial and transient patterns on electrodes. *J. Chem. Phys.* **137**, 014504 (2012)
- Jasik-Ślęzak, J., Olszówka, K., Ślęzak, A.: Estimation of thickness of concentration boundary layers by osmotic volume flux determination. *Gen. Physiol. Biophys.* **30**, 186–195 (2011)
- Kargol, M.: The gravimetric hypothesis of xylem transport of water in plants. *Gen. Physiol. Biophys.* **11**, 469–487 (1992)
- Kargol, A.: Modified Kedem–Katchalsky equations and their application. *J. Membr. Sci.* **174**, 43–53 (2000)
- Katchalsky, A., Curran, P.F.: *Nonequilibrium Thermodynamics in Biophysics*. Harvard, Cambridge (1965)
- Kedem, O., Katchalsky, A.: Thermodynamic analysis of the permeability of biological membranes to non-electrolytes. *Biochim. Biophys. Acta* **27**, 229–246 (1958)
- Kondepudi, D., Prigogine, I.: Sensitivity of nonequilibrium systems. *Phys. A* **107**, 1–24 (1981)
- Kondepudi, D.: *Introduction to Modern Thermodynamics*. Wiley, Chichester (2008)
- Landau, L., Lifshitz, E.: *Fluid Mechanics*. Pergamon Press, Oxford (1987)
- Larchet, C., Nouri, S., Auclair, B., Dammak, L., Nikonenko, V.: Application of chronopotentiometry to determine the thickness of diffusion layer adjacent to an ion-exchange under natural convection. *Adv. Colloid Interface Sci.* **139**, 45–61 (2008)
- Mishchuk, N.A.: Concentration polarization of interface and non-linear electrokinetic phenomena. *Adv. Colloid Interface Sci.* **160**, 16–39 (2010)
- Moya, A.A., Horno, J.: Study of the linearity of the voltage–current relationship in ion-exchange membranes using the network simulation method. *J. Membr. Sci.* **235**, 123–129 (2004)
- Nield, D.A., Bejan, A.: *Convection in Porous Media*. Springer, New York (2006)
- Nikonenko, V., Pismenskaya, N.D., Belova, E.I., Sizat, P., Huguette, P., Pourcelly, G., Larchet, C.: Intensive current transfer in membrane systems: modelling, mechanism and application in electro dialysis. *Adv. Colloid Interface Sci.* **160**, 101–123 (2010)
- Normand, C., Pomeau, Y., Velarde, M.Y.: Convective instability: a physicist's approach. *Rev. Mod. Phys.* **49**, 581–624 (1977)
- Pappenheimer, J.R.: Role of pre-epithelial ‘unstirred’ layers in absorption of nutrients from the human jejunum. *J. Membr. Biol.* **179**, 185–204 (2001)
- Peusner, L.: *The principles of network thermodynamics and biophysical applications*. PhD thesis, Harvard, Cambridge (1970)
- Peusner, L.: Hierarchies of irreversible energy conversion systems: a network thermodynamics approach. I. Linear steady state without storage. *J. Theor. Biol.* **102**, 7–39 (1983a)
- Peusner, L.: Hierarchies of irreversible energy conversion systems. II. Network derivation of linear transport equations. *J. Theor. Biol.* **115**, 319–335 (1985a)
- Peusner, L.: *Studies in Network Thermodynamics*. Elsevier, Amsterdam (1986)
- Prigogine, I.: *The End of Certainty: Time, Chaos and the New Laws of Nature*. The Free Press, New York (1997)
- Puthenveetil, B.A., Arakeri, J.H.: Convection due to an unstable density difference across a permeable membrane. *J. Fluid Mech.* **609**, 139–170 (2008)
- Puthenveetil, B.A., Gunasegarane, G.S., Agrawal, Y.K., Arakeri, J.H.: Length of near-wall plumes in turbulent convection. *J. Fluid Mech.* **685**, 335–364 (2011)
- Ramareddy, G.V., Puthenveetil, B.A.: The $Pe \sim 1$ regime of convection across a horizontal permeable membrane. *J. Fluid Mech.* **679**, 476–504 (2011)
- Rubinstein, I., Zaltzman, B.: Electro-osmotically induced convection at a permselective membrane. *Phys. Rev. E* **62**, 2238–2251 (2000)
- Salcedo-Diaz, R., García-Algado, P., García-Rodríguez, M., Fernández-Sempere, J., Ruiz-Breviá, F.: Visualization and modeling of the polarization layer in crossflow reverse osmosis in a silt-type channel. *J. Membr. Sci.* **456**, 21–30 (2014)
- Serna, J., Velasco, J.S., Soto Meca, A.: Application of network simulation method to viscous flows: the nanofluid heated lid cavity under pulsating flow. *Comput. Fluids* **91**, 10–20 (2014)
- Shachar-Hill, B., Hill, A.E.: Convective fluid flow through the paracellular system of Nectorius gall-bladder epithelium as revealed by dextran probes. *J. Physiol.* **468**, 463–486 (1993)
- Schlichting, H., Gersten, K.: *Boundary Layers Theory*. Springer, Berlin (2000)
- Ślęzak, A., Dworecki, K., Anderson, J.E.: Gravitational effects on transmembrane flux: the Rayleigh–Taylor convective instability. *J. Membr. Sci.* **23**, 71–81 (1985)
- Ślęzak, A.: Irreversible thermodynamic model equations of the transport across a horizontally mounted membrane. *Biophys. Chem.* **34**, 91–102 (1989)

- Ślęzak, A., Grzegorzczyn, S., Jasik-Ślęzak, J., Michalska-Małecka, K.: Natural convection as an asymmetrical factor of the transport through porous membrane. *Transp. Porous Media* **84**, 685–698 (2010)
- Ślęzak, A., Grzegorzczyn, S., Batko, K.M.: Resistance coefficients of polymer membrane with concentration polarization. *Transp. Porous Media* **95**, 151–170 (2012)
- Ślęzak, A., Dworecki, K., Ślęzak, I.H., Wąsik, S.: Permeability coefficient model equations of the complex: membrane-concentration boundary layers for ternary nonelectrolyte solutions. *J. Membr. Sci.* **267**, 50–57 (2005)
- Ślęzak, A., Jasik-Ślęzak, J., Grzegorzczyn, S., Ślęzak-Prochazka, I.: Nonlinear effects in osmotic volume flows of electrolyte solutions through double-membrane system. *Transp. Porous Media* **92**, 337–356 (2012)
- Wang, J., Dlamini, D.S., Mishra, A.K., Pendergast, M.T.M., Wong, M.C.Y., Mamba, B.B., Freger, V., Verliefde, A.R.D., Hoek, E.M.V.: A critical review of transport through osmotic membranes. *J. Membr. Sci.* **454**, 516–537 (2014)
- Ward, W.J., Le Blanc, O.H.: Rayleigh–Benard convection in an electrochemical redox cell. *Science* **225**, 1471–1472 (1984)